Sustainable Energy & Fuels

Artificial Foliage with Remarkable Quantum Conversion Efficiency in Bicarbonate to Formate

Journal:	*Sustainable Energy & Fuels*
Manuscript ID	SE-COM-08-2021-001307.R1
Article Type:	Communication
Date Submitted by the Author:	02-Nov-2021
Complete List of Authors:	Pan, Hanqing; New Mexico Institute of Mining and Technology, Chemistry Premachandra, Dumindu; New Mexico Institute of Mining and Technology, Chemistry Heagy, Michael; Rochester Institute of Technology College of Science, Chemistry

COMMUNICATION

Artificial Foliage with Remarkable Quantum Conversion Efficiency in Bicarbonate to Formate

Hanqing Pan[a], Dumindu Premachandra[a], and Michael D. Heagy[b*]

Received 00th January 20xx,
Accepted 00th January 20xx
DOI: 10.1039/x0xx00000x

Abstract: An efficient heterogeneous immobilized device for the photoreduction of bicarbonate to formate was achieved by a thin-film semiconductor with metallophthalocyanines. The two-layer devices were fabricated by the deposition of (TiO_2 or Cu_2O) and zinc or cobalt phthalocyanines as photosensitizer onto an SiO_2 disc.

In the development of solar fuels, practical devices that can exceed the efficiency of natural photosynthesis, where up to 1% of incident sunlight converts to biomass, are expected to rival Nature.[1] The usual approach in solar-driven photochemistry involves a flask or test tube under one sun, where issues such as photon efficiency and the tendency of particles to agglomerate in water, limit potential scale-up. Light penetration becomes a particularly important aspect in photoredox catalysis. Semiconductor particles typically possess high extinction coefficients and the Bouguer-Lambert-Beer law limits light penetration to the outer layer of the reaction vessel.[2] By comparison, semiconductor thin-films have high catalytic value, since the semiconductor material remains immobilized on the surface.[3] To improve efficiency, metallophthalocyanine (MPc) dyes feature electron-injecting properties under visible light and demonstrate potential as light-harvesting components in dye-sensitized titania.[4] As photostable and thermally robust chromophores, electron transfer occurs through changes in the oxidation state of the metal cations, whereby a nuclear center such as cobalt can shift alternatively from +2 to +3.[5,6] Recently, MPc's have been mixed via organically-modified silicate thin-films doped with Cu(II), Fe(II), and Fe(III) as photocatalytic devices for oxidative degradation of organic pollutants.[7a-d]

Because less than 1% of total dissolved inorganic carbon is unionized CO_2, the world's oceans can be considered as a dilute solution (~2 mmol/kg) of sodium bicarbonate.[8] Therefore, we have applied a number of earth-abundant, non-toxic photocatalysts, with different sizes and shapes to convert bicarbonate to formate.[9-16] Methanoic acid is an intermediate toward methanol production, and is used in a number of industrial, medical, and agricultural applications. Formate serves as a hydrogen donor in fuel cells, thereby making the chemistry both regenerative and sustainable.[17]

Based on these considerations, we report results from zinc and cobalt phthalocyanines, utilized in conjunction with semiconductor photocatalysts in a foliated device. Given the proximity of their LUMO energies to the conduction band of TiO_2, among different metal centers, these MPc systems were hypothesized to be particularly effective toward electron injection.[18] With the advantages of a maximized surface area, while preventing the agglomeration of a semiconductor suspension, this artificial foliage offers the potential of extended optical absorption, increased overall supply of electrons in the conduction band, and an efficient hole scavenger that delays charge carrier recombination. Among the two designs, the device constructed with layers of CoPc and TiO_2 (Figure 1) exhibited the highest photocatalytic activity with solar to chemical energy conversion efficiency reaching 0.12%.

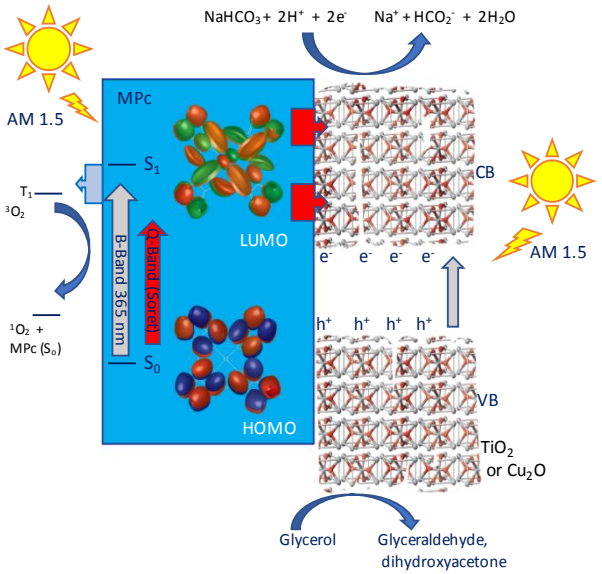

Figure 1. Schematic of the electron-transfer and redox chemical pathways via solar irradiation using semiconductor and MPc on quartz disc.

[a] *New Mexico Institute of Mining & Technology, Socorro, NM USA*
[b] *Rochester Institute of Technology, Rochester, NY USA*
Electronic Supplementary Information (ESI) available: [details of any supplementary information available should be included here]. See DOI: 10.1039/x0xx00000x

COMMUNICATION

In the foliated design, we envisioned a reaction pathway whereby a cooperative electron-transfer effect exists between the semiconductor and MPc (Figure. 1). Incident photons excite TiO_2 valence band electrons to the conduction band, which subsequently reduce bicarbonate to formate. The photogenerated holes proceed to oxidize glycerol to glyceraldehyde and dihydroxyacetone. Concomitantly, photocatalytic activity is enhanced by the phthalocyanine sensitizer, through absorption of photons in the visible region. The photoexcitation of the sensitizer excites electrons from the S_0 ground state to an S_1 state, where it is injected into the conduction band of TiO_2, a faster process than direct relaxation back to the ground state. Highly active species such as $^{\bullet}OH$ and $O_2^{\bullet-}$ are generated at the TiO_2 surface; albeit low O_2 concentrations relative to HCO_3^-, and thereby impede electron/hole recombination.[6]

The devices comprised of MPc photosensitizers at less than 100 nm thick, and semiconductors (also < 100 nm) were characterized by solid-state UV-Vis absorption. Diffuse reflectance spectroscopy data (Supplementary Information, figure S7) show that zinc phthalocyanine exhibits the two intense peaks at 375 nm typical of the Soret band (B-band) and 700 nm (Q-band), whereas cobalt phthalocyanine displays two peaks at 300 nm (B-band) and 600 nm (Q-band), with a shoulder peak at 700 nm. Because the TiO_2 band gap is larger than the energy for an MPc π-π^* electron transition, the semiconductor typically shows no significant absorbance for visible light and exhibits only a fundamental absorption band in the UV region. Cu_2O possesses a smaller band gap than TiO_2, so it effectively absorbs in the visible region. Kubelka-Munk treated plots (SI) indicate that the band gap energies for TiO_2, Cu_2O, ZnPc, and CoPc are 3.2, 1.8, 1.9, and 1.6 eV, respectively. With the addition of MPc, the band gap energy of TiO_2 decreases slightly to 2.9 eV resulting from the electronic coupling, which is consistent with previous literature citing 2.97 eV.[6]

Absorption spectrophotometric investigations in solution support these sold-state optical features when phthalocyanines of either cobalt or zinc were adsorbed or suspended with either metal oxide. In the case of ZnPc adsorbed onto Cu_2O, a 10 nm blue shift occurs) in the Soret band (B-band) and another 10 nm blue shift happens at 700 nm (Q-band). While similar wavelength shifting was noted in the B-band for ZnPc with TiO_2, significant spectral broadening and an additional peak appears in the Q-band region. For CoPc similar but smaller blue shifts trends of 5 nm were observed with both B- and Q-bands when deposited onto the Cu_2O substrate. To study the photo-induced behavior of ZnPc in the absence and presence of Cu_2O and TiO_2, steady-state fluorescence measurements are carried out in toluene. Given the paramagnetic nature of the nuclear center, CoPc does not fluoresce. Instead of stimulated emission, this MPc is susceptible to energy transfer.[19] As shown in the SI section, the fluorescence intensity of ZnPc undergoes a marked decrease in the presence of TiO_2 NPs and to a lesser extent with Cu_2O. The fluorescence quenching of ZnPc in the company of Cu_2O or TiO_2 may be attributed to energy transfer from photoexcited MPc to NP semiconductors.[20-22]

Electron transfer at the interface of a photoactive species and the semiconductor surface is a fundamental aspect for organic semiconductor devices.[23,24] In particular, ultrafast charge-separation led by electron injection from electronically excited photoactive molecules to the conduction band of a wide band gap semiconductor are key steps toward improving the performance of these materials.[25-27] Cyclic voltammetry was used to place band gap values on an absolute NHE scale (details of analysis in supplementary info). Cu_2O and TiO_2 showed band gaps of 2.0 and 3.23 eV, respectively; and both phthalocyanines exhibited band gap values of 1.6 eV (SI). Contact between TiO_2 and ZnPc generally involves a redistribution of electronic charge. The ZnPc oxidation potential of S_0, S_1, and T_1 are 1.18, -0.63, and -0.02 eV respectively. $ZnPc^+$ is located 0.2 eV below the CB edge of TiO_2, and the energy of S_1 is higher than the CB of TiO_2, but the energy of T_1 is lower than CB of TiO_2, therefore it is thermodynamically feasible for electron transfer from the S_1 state to the CB of TiO_2 as ZnPc photo-oxidizes to $ZnPc^+$.[28,29]

Figures 2a and 2b show that formate production increases linearly as a function of time in both the control experiments and in the double thin-film devices. Table 1 and Figure 3 display averaged results of formate productivity from the photocatalytic reduction of bicarbonate. Control experiments 1 and 2, respectively with Cu_2O and TiO_2 in solution were conducted with semiconductors as a suspension in the aqueous phase and sensitizer as a thin film, which resulted in lower formate production. Cu_2O and TiO_2 in solution alone resulted in 7.56 and 14.67 µmol formate, which increased when a layer of sensitizer was added. However, due to the minimal contact between semiconductor and sensitizer, we have constructed our device to have two thin films of semiconductor and sensitizer with intimate contact.

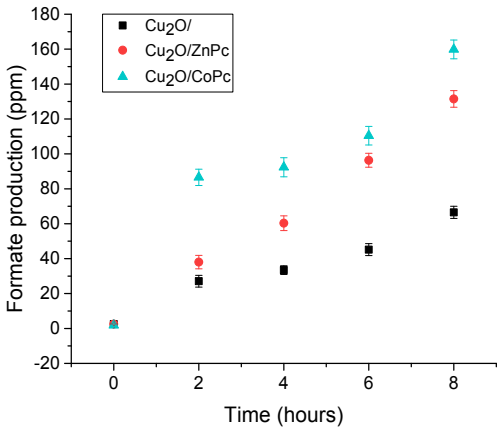

COMMUNICATION

Figure 2a. Formate production in ppm from the devices using Cu_2O and MPc. Reaction conditions: aerobic, RT, pH = 8.5 (sodium saturated bicarbonate), irradiation condition = AM 1.5, one sun, 100 mW/cm^2 with glycerol as reducing agent.

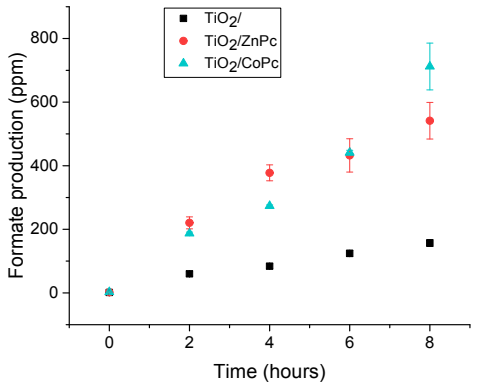

Figure 2b. Formate production in ppm from the devices using TiO_2 and MPc. Reaction conditions identical to Figure 2a.

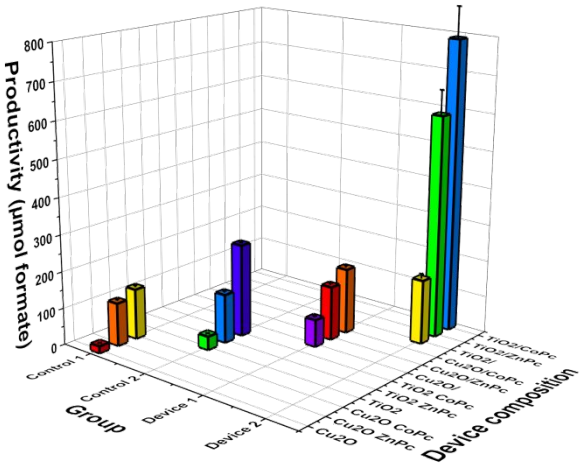

Figure 3. Formate productivity (in µmol formate) of the control experiments and devices.

Even without sensitizer, thin-film Cu_2O (denoted Cu_2O/) and TiO_2 (denoted TiO_2/) reached 29.3 and 69.3 µmol formate, respectively, presumably due to the increase in surface area and contact with bicarbonate. At this preliminary stage, photocatalytic contribution by the semiconductor cannot be excluded. Device 1 used layers of Cu_2O and zinc or cobalt phthalocyanine, which resulted in an enhancement in productivity when compared to the control experiment with Cu_2O. Device 2 consisted of thin-film TiO_2 and sensitizer (denoted TiO_2/ZnPc and TiO_2/CoPc) reached peak formate productivity of 240.4. and 316.4 µmol formate for zinc and cobalt phthalocyanine, respectively. Turnover numbers for ZnPc and CoPc were calculated approximately to be 106 and 145, respectively (full details in SI; Table S2). Formate production can be quantified in terms of Apparent Quantum Efficiency (AQE). The highest AQE is observed in Device 2 with TiO_2 and cobalt phthalocyanine configuration reaching 0.12% (Table 1).

Table 1. Productivity and apparent quantum efficiency (AQE) of control experiments and devices

Trial	Layer orientation	Productivity (µmol formate)	AQE (%)
Control 1	Cu_2O	7.6 ± 0.12	2.0 x 10^{-3} ±0.003
	Cu_2O ZnPc	46.7 ± 2.2	1.3 x 10^{-2} ±0.062
	Cu_2O CoPc	54.7 ± 2.1	1.5 x 10^{-2} ±0.058
Control 2	TiO_2	14.7 ± 0.4	5.7 x 10^{-2} ±0.014
	TiO_2 ZnPc	52.9 ± 2.3	2.1 x 10^{-2} ±0.084
	TiO_2 CoPc	100.4 ± 1.2	3.9 x 10^{-2} ±0.047
Device 1	Cu_2O/	29.3 ± 1.5	8.0 x 10^{-3} ±0.041
	Cu_2O/ZnPc	58.2 ± 2.1	1.6 x 10^{-2} ±0.059
	Cu_2O/CoPc	70.7 ± 2.4	1.9 x 10^{-2} ±0.064
Device 2	TiO_2/	69.3 ± 4.8	2.7 x 10^{-2} ±0.18
	TiO_2/ZnPc	240.4 ± 25.6	8.9 x 10^{-2} ±0.94
	TiO_2/CoPc	316.4 ± 32.7	1.2 x 10^{-1} ±0.12

*All reported values and error are averaged from triplicate measurements.

In most cases the electrons and holes recombine too rapidly for the semiconductor to be efficient. Rapid charge carrier recombination can be mitigated by the addition of a hole scavenger, a sacrificial agent that undergoes oxidation in the photocatalytic process.[30] Hole scavengers are critical elements in photocatalytic reactions because they have been reported to enhance the photoactivity of TiO_2.[31-34] In this work we highlight glycerol as a hole scavenger because it is derived from non-petroleum sources and can be synthesized biologically. The superiority of glycerol as a hole scavenger can be explained by the fact that glycerol possesses more primary OH groups, which leads to the improved C-H hole scavenging reactivity. Glycerol has three hydroxyl groups and can be adsorbed more strongly on TiO_2 or Cu_2O in comparison to 2-propanol. Additionally, polyhydroxyls such as adsorbed glycerol appear to favor efficient hydride transfer to photo-generated holes in TiO_2 thereby suppressing the charge carrier recombination.[35] Taking into account the importance of recyclability of photocatalysts, we examined the recycling of the devices during two cycles. At this time, the phthalocyanine layer can wash off after

COMMUNICATION

being in contact with the glycerol buffer, thus showing the decrease in intensity in UV-Vis (Supplementary Information Fig S13). But we were pleased to report that there was no significant change in productivity in the second cycle (Supplementary Information Fig S14).

Conclusions

In summary, a novel foliated device was constructed with a semiconductor layer and photosensitizer layer onto a quartz platform. Photoreduction of bicarbonate to formate approached 3x higher yield of photoconversion than that of suspended photocatalyst. We attribute these extraordinary results to the synergistic, foliated design of the positive hole scavenger and photosensitizer. The photo-excited phthalocyanines can transfer its electrons into the conduction band of the semiconductor, enhancing the overall electron supply. To summarize these two device design concepts, MPc was first deposited onto SiO_2 discs, and then TiO_2 or Cu_2O. The photoreduction is expected to occur on the surface of the TiO_2/Cu_2O where the HCO_3^-/glycerol mixture interface. TiO_2 is a known catalyst for photoreduction of HCO_3^- to HCO_2^- however due to the higher band gap energy (3.2 eV) it requires light in the UV region to excite an electron from VB to CB. Thus MPc, as a visible light active photosensitizer, injects photo-excited electrons to the CB of TiO_2 where the photoreduction occurs. Our future studies focus on transient absorption spectroscopy to confirm the charge transfer mechanism from MPc to CB of TiO_2. As demonstrated here, thin films in the form of artificial foliage are of high practical value because the immobilization of TiO_2 prevents agglomeration and maximizes surface area which allows for more bicarbonate adsorption and greater solar penetration. The ability to create the thin films via thermally depositing the photosensitizer and semiconductor allows for uniform layers without wasting material. Future investigations include isotope labeling to confirm the source of formate, and permeable biopolymer coatings for continuous workability. In closing, these findings offer progress toward CO_2 mitigation via negative emission technologies. With bicarbonate as the predominant dissolved carbon species in a marine environment, a recent study has identified the large potential scalability of solar islands toward solar fuel generation.[36,37]

Conflicts of interest

The authors declare no competing financial interest.

Notes and references

1. Jacobsson, T. J.; Fjallstrom, V.; Sahlberg, M.; Edoff, M.; Edvinsson, T. *Energy Env. Sci.* **2013,** *6* (12), 3676-3683.
2. Cambié, D.; Zhao, F.; Hessel, V.; Debije Michael, G.; Noël, T., *Angew. Chem. Int. Ed.* **2016,** *56* (4), 1050-1054.
3. Zhou, H.; Fan, T.; Li, X.; Zhang, D.; Guo, Q.; Ogawa, H., *J. Mater. Chem.* **2009,** *19*, 2695-2703.
4. Mele, G.; Annese, C.; Accolti, L.; De Riccardis, A.; Fusco, C.; Palmisano, L.; Scarlino, A.; Vasapollo, G., *Molecules,* **2015,** *20*, 396-415.
5. Mele, G.; Del Sole, R.; Vasapollo, G.; García-López, E.; Palmisano, L.; Schiavello, M. *J. Catal.* **2003,** *217* (2), 334-342.
6. Ebrahimian, A.; Zanjanchi, M. A.; Noei, H.; Arvand, M.; Wang, Y. *J. Environ. Chem. Eng.* **2014,** *2* (1), 484-494.
7. (a) Palmisano, G.; Gutiérrez, M. C.; Ferrer, M. L.; Gil-Luna, M. D.; Augugliaro, V.; Yurdakal, S.; Pagliaro, M., *J. Phys. Chem. C.* **2008,** *112* (7), 2667-2670. (b) Koodali, T.; Wilner, I.;Bossmann, S.; Braun, A. *J. Phys. Chem. B.* **1998**, *102,* 9397-9403. (b) Mahmiani, Y.; Sevim, A.M.; Gül, A. *J. Photochem. Photobiol. A: Chem.* **2016**, *321*, 24-32. (c) Pirbazari, A.E.; *Proc. Mater. Sci.* **2015**, *5*, 622-627. (d) Henderson, M.A. *Surf. Sci. Reports,* **2011**, *66*, 185-297.
8. Dickson, A.G., Part 1: Seawater Carbonate Chemistry, The carbon dioxide system in seawater: equilibrium chemistry and measurements. *Guide to best practices for ocean acidification research reporting*, 2010. Luxembourg: Publications Office of the EU.
9. Pan, H. M., K.; Heagy, M.D. *Top. Catal.* **2018,** *61*, 601-609.
10. Leonard, D. P. P., H.; Heagy, M.D., *ACS Appl. Mater. Inter.* **2015,** *7*, 24543-24549.
11. Pan, H. R., V.; Martindale, K.; Heagy, M.D., *ACS Sust. Chem. Eng.* **2019,** *7*, 1210-1219.
12. Pan, H.; Steininger. A.; Heagy, M.D.; Chowdhury, S., *J. CO_2 Util.,* **2017,** *22C*, 117-123.
13. Pan. H.; Chowdhury, S. Premachandra, D.; Olguin, S; Heagy, M.D., *ACS Sust. Chem. Eng.* **2018,** *6*, 1872-1880.
14. Pan, H.; Heagy, M.D. *MRS Adv.* **2019,** *4*, 425-433.
15. Pan, H.; Rajapaksha, R.; Heagy, M.D., *MRS Adv.* **2019,** *4*, 2638-2643.
16. Beierle, A.; Gieri, P.; Pan, H.; Heagy, M.D.; Manjavacas, A.; Chowdhury, S. *Solar Energy Mat. Solar Cells,* **2019,** *200*, 109967.
17. Pan, H., Heagy, M.D. *Nanomaterials,* **2020**, 10, 2422.
18. Pan.H.; Heagy, M.D. *MRS Commun.* **2018**, 8, 1173-1177.
19. Liao, M.-S.; Scheiner, S. *J. Chem. Phys.* **2001**, *114*, 9780-9791.
20. Ray, A.; Bhattacharya, S. *Chem. Phys. Lett.* **2016,** *651*, 66-71.
21. Vallejo, W.; Diaz-Uribe, C.; Cantillo, A., *J. Photochem. Photobio. A: Chem.* **2015,** *299*, 80-86.
22. Sharma, G. D.; Kumara, R.; Roy, M. S.,*Solar Energy Mater. Solar Cells* **2006,** *90*, 32-45.
23. Grätzel, M., Photoelectrochemical cells. *Nature* **2001,** *414*, 338.
24. Ino, D.; Watanabe, K.; Takagi, N.; Matsumoto, Y. *J. Phys. Chem. B,* **2005,** *109* (38), 18018-18024.
25. Rehm, J. M.; McLendon, G. L.; Nagasawa, Y.; Yoshihara, K.; Moser, J.; Grätzel, M., *J. Phys. Chem.* **1996,** *100* (23), 9577-9578.
26. Nazeeruddin, M. K.; Kay, A.; Rodicio, I.; Humphry-Baker, R.; Mueller, E.; Liska, P.; Vlachopoulos, N.; Graetzel, M. *J. Am. Chem. Soc.* **1993,** *115* (14), 6382-6390.
27. Asbury, J. B.; Hao, E.; Wang, Y.; Ghosh, H. N.; Lian, T., *J. Phys. Chem. B.* **2001,** *105* (20), 4545-4557.
28. Zhao, Z.-H.; Fan, J.-M.; Wang, Z.-Z., *J. Cleaner Prod.* **2007,** *15* (18), 1894-1897.

COMMUNICATION

29. Liu, S.; Zhao, Z.; Wang, Z., *Photochem. Photobiol. Sci.* **2007,** *6* (6), 695-700.
30. Berr, M. J.; Wagner, P.; Fischbach, S.; Vaneski, A.; Schneider, J.; Susha, A. S.; Rogach, A. L.; Jäckel, F.; Feldmann, J., *Appl. Phys. Lett.* **2012,** *100* (22), 223903.
31. Murcia, J. J.; Hidalgo, M. C.; Navío, J. A.; Vaiano, V.; Ciambelli, P.; Sannino, D. *Catal. Today,* **2012,** *196* (1), 101-109.
32. Qin, S.; Xin, F.; Liu, Y.; Yin, X.; Ma, W., *J. Coll. Inter. Sci.* **2011,** *356* (1), 257-261.
33. Fujiwara, H.; Hosokawa, H.; Murakoshi, K.; Wada, Y.; Yanagida, S.; Okada, T.; Kobayashi, H., *J. Phys. Chem. B* **1997,** *101* (41), 8270-8278.
34. Kim, G.; Choi, W., *Appl. Catal. B: Env.* **2010,** *100* (1), 77-83.
35. Zhou, B.; Song, J.; Zhou, H.; Wu, L.; Wu, T.; Liu, Z.; Han, B., *RSC Adv.* **2015,** *5* (46), 36347-36352.
36. Patterson, B. D.; Mo, F.; Borgschulte, A.; Hillestad, M.; Joose, F.; Kristiansen, T.; Sunde, S.; van Bokhoven, J. A. *PNAS*, **2019**, 116, 12212-12210.
37. Roy, N.; Suzuki, N.; Terashima, C.; Fujishima, A. *Bull. Chem. Soc. Jpn*. **2019**, 92, 178-19

